Utrecht University

Depart of Earth Sciences
Paleomagnetic laboratory
Fort Hoofddijk

MAGNETIC MINERALOGY OF HOLOCENE SEDIMENTS FROM LAKE IJSSEL, NETHERLANDS

greigite formation in ancient levee systems

V.A.M. Schmits, M.J. Dekkers, K.M. Cohen

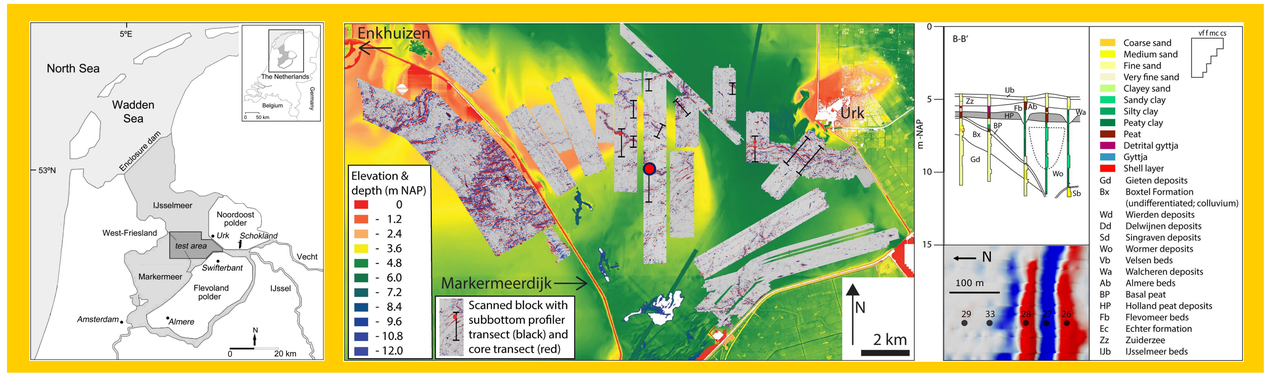

Figure 1 – Left: location of the IJsselmeer, test area in dark grey. Middle: the magnetic lineations recorded in the IJsselmeer plotted on a topographic map, core VC-26 marked with red dot. Right: detailed view of core VC-26 within the levee system and schematic cross section of the levee. All three figures are adapted from [1].

Surprising magnetic lineations

An extensive magnetometer survey of the lake bottom has revealed curvy magnetic lineations evocative of relatively small natural channels (fig. 1)[1]. To investigate the source of the magnetic signal, and to further our understanding of the geologic past, piston cores of ~7 m long were recovered[1]. Magnetically susceptible Middle Holocene levee clays with some more sand-rich layers in between are studied (Fig. 2A). Previous research indicated the presence of the ferrimagnetic mineral greigite (Fe_3S_4) [2]. It was unclear whether this greigite would have formed syn- or post-depositionally in the sediment, and the formation mechanism of the greigite remains ambiguous. With greigite potentially being formed later, a paleosecular variation (PSV) curve would become unreliable.

This study, focused on natural levee core VC-26, aims to recover the depositional history of the magnetic minerals and to confirm the presence of greigite. The magnetic susceptibility was recorded on the surface of the split core, and subsequently samples were taken at ~1.5 cm intervals. The natural remanent magnetization (NRM) was demagnetized with alternating fields (AF). Acquisition curves of the anhysteretic and isothermal remanent magnetization (ARM & IRM) were measured on all samples. IRM curve fitting was performed on all individual samples[5]. End member modelling was done with the whole IRM acquisition curve data set[7]. Specific samples were selected for thermomagnetic runs ,first-order-reversal-curve (FORC) analysis, and Scanning Electron Microscopy (SEM) imagery.

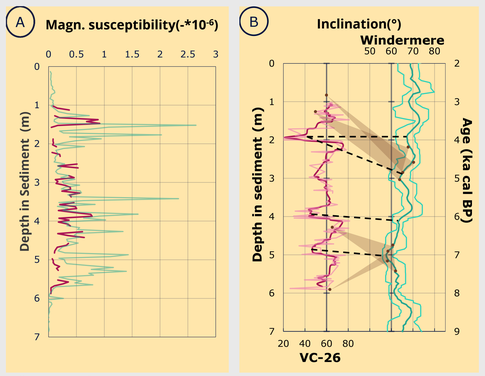

Figure 2 – Core VC-26 A: magnetic susceptibility and B: Inclination. VC-26 data is in purple (data points are light shaded, moving average trend is darker shaded). Compared to (in teal) A: 2021 measurements[2]. B: stacked curves of Windermere[3] with calibrated age in ka. Calibrated C-14 ages (by [1]) are included in brown. Potential preliminary age estimates in black.

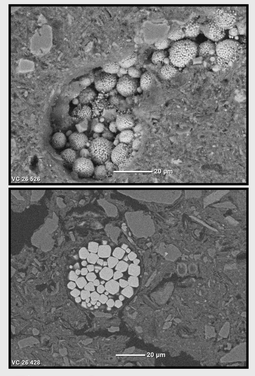

Figure 3 –Tabletop SEM imagery of samples 526 (top) and 428 (bottom). framboids of euhedral cubic pyrite.

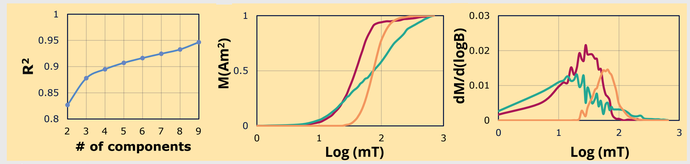

Figure 4 – End member modelling results. From left to right: R^2 plot for multiple endmembers, Linear acquisition plot (LAP), and Gradient acquisition plot (GAP) for 3 members: EM-1 (purple), EM-2 (teal), and EM-3 (orange).

Figure 5 – End member contributions for the 3-end member model. Depth is in cm, colours are the same as in figure 4. Gaps are due to the non availability of material at these depths.

Paleosecular variation and End member modelling

The NRM of 117 data points was deemed consistent enough to reconstruct the inclination and declination and generate a PSV record[7] (fig. 2) which was compared to the geographical relatively close Windermere curve from the UK[3]. The declination curve was deemed unreliable and is not shown, because the core is not azimuthally oriented. With the C-14 ages (in brown in fig. 2) as rough guide to the ages of magnetic signal, inclinations of the Windermere curve seems slightly higher than in VC-26, possibly related to Windermere's more northern latitude. Firm corelation is however tedious: particularly the inclination lows in VC-26 (20°-40°) are not typical for this latitude and absent in the Windermere curve. Inclination and declination(not shown) seem affected by some rotation during core retrieval, as values trend downward within most core sections.

Looking at the R^2 plot in figure 4, a three-end-member model is optimal. EM-1 and EM-3 are well defined in LAP/GAP plots and can be used to define magnetic components. EM-2 is an amalgamation of the of the remaining magnetic material and is only significantly present in the sandy parts of the core with a much weaker magnetic signal (fig. 5). The IRM components[5] of samples at 428 and 137 cm are slightly different (left-most panels in fig. 6). Both peaks (blue curves) could still be greigite derived, but hint at a potentially different origin. The curve in sample 428 can be linked to EM-1 in figure 4 and the main (blue) curve for sample 137 is EM-3.

SEM imagery of VC-26 samples is shown in figure 3. Framboidal structures up to 30 µm, with microcrystalline euhedral cubic crystals of 3-10 µm. The framboids are expected to be mainly pyrite, of which diagenetic greigite is a precursor, hinting that at least some secondary greigite is present. It doesn't exclude the presence magnetotactic greigite, as these crystals are too small for tabletop SEM detection.

Thermomagnetic, IRM curves, FORCs, and preliminary conclusions

The thermomagnetic runs (in air) indicate that greigite is breaking down (fig. 6, right-most panels). Around 480 °C the magnetization peaks indicate the oxidation of non-magnetic iron-sulphide species to magnetic iron oxide species, likely pyrite to magnetite. The difference between the 2021 (teal) and 2023 (purple) measurements for 428 is peculiar as one anticipates the greigite signal to go down over time instead of up.

In the FORC diagram (fig. 6, central panels) both samples feature a prominent central ridge, but in sample 137 there is also a peak just below the centre. The central ridge expresses non-interacting single domain (SD) behaviour, and together with the IRM acquisition curves and thermomagnetic data, this greigite seems from magnetotactic bacterial origin. The second peak in sample 137 is an indicator of more magnetic interactions which is typical of authigenic greigite.

Carefully we may say that even when secondary greigite is present in VC-26, the signal is still dominated by quickly formed SD magnetotactic greigite and thus ages of the PSV curve should roughly match the age of sediment deposition, i.e. ~7.5 to 4.2 ka BP at maximum, and potentially ~7-5 ka BP with a faster deposition (as indicated in fig. 2B).

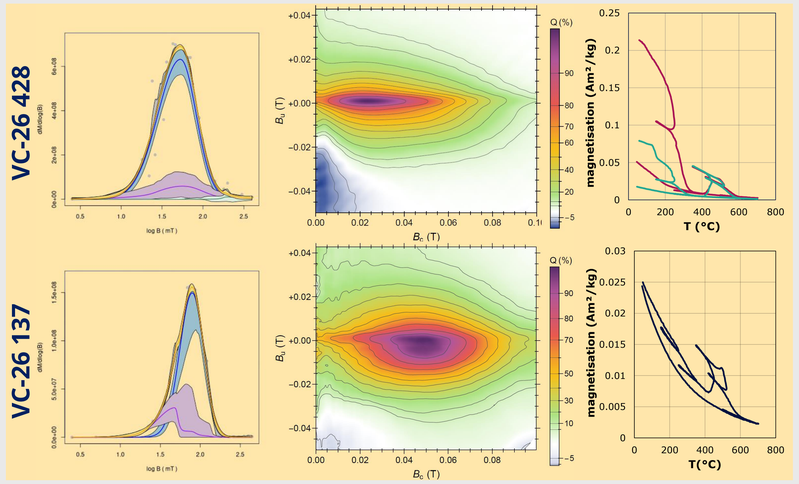

Figure 6 – Analysis of VC-26 samples 428 (top) and 137 (bottom), from left to right: coercivity components fitted to IRM acquisition curves with the main component in blue, quantitative FORC diagrams, and thermomagnetic runs where sample 428 (purple) is also compared to a previous measurement in 2021 (teal).

References

1. van den Brenk, S., Huisman, H., Willemse, N. W., Smit, B., & van Os, B. J. H. (2023). Magnetometer mapping of drowned prehistoric landscapes for Archaeological Heritage Management in the Netherlands. Archaeological Prospection.
2. van Aalst, W. (2022) Magnetic Lineations in the Lake Ijssel (master thesis)
3. Avery, R. S., Xuan, C., Kemp, A. E. S., Bull, J. M., Cotterill, C. J., Fielding, J. J., Pearce, R. B., & Croudace, I. W. (2017). A new Holocene record of geomagnetic secular variation from Windermere, UK. Earth and Planetary Science Letters, 477, 108–122.
4. Maxbauer, D. P., Feinberg, J. M., & Fox, D. L. (2016). MAX UnMix: A web application for unmixing magnetic coercivity distributions. Computers and Geosciences, 95, 140–145.
5. Egli, R. (2013). VARIFORC: An optimized protocol for calculating non-regular first-order reversal curve (FORC) diagrams. Global and Planetary Change, 110, 302–320.
6. Weltje G.J. , (1997). End-member modeling of compositional data: numerical-statistical algorithms for solving the explicit mixing problem, Math. Geol., 29, 503–549
7. Koymans, M. R., van Hinsbergen, D. J. J., Pastor-Galán, D., Vaes, B., & Langereis, C. G. (2020). Towards FAIR paleomagnetic data management through Paleomagnetism. org 2.0. Geochemistry, Geophysics, Geosystems, 21(2), e2019GC008838

/forthoofddijk.geo.uu.nl